optica

Spectral vector beams for high-speed spectroscopic measurements

Lea Kopf,[1] Juan R. Deop Ruano,[1] Markus Hiekkamäki,[1] Timo Stolt,[1] Mikko J. Huttunen,[1] Frédéric Bouchard,[2] and Robert Fickler[1,*]

[1]Tampere University, Photonics Laboratory, Physics Unit, Tampere, FI-33014, Finland
[2]National Research Council of Canada, 100 Sussex Drive, Ottawa, Ontario K1A 0R6, Canada
*Corresponding author: robert.fickler@tuni.fi

Received 12 March 2021; revised 11 May 2021; accepted 22 May 2021 (Doc. ID 424960); published 17 June 2021

Structuring light in multiple degrees of freedom has become a powerful approach to create complex states of light for fundamental studies and applications. Here, we investigate the light field of an ultrafast laser beam with a wavelength-dependent polarization state, which we term a spectral vector beam. We present a simple technique to generate and tune such structured beams and demonstrate their spectroscopic capabilities. By measuring only the polarization state using fast photodetectors, it is possible to track pulse-to-pulse changes in the frequency spectrum caused by, e.g., narrowband transmission or absorption. In our experiments, we reach readout rates of around 6 MHz, which is limited by our technical ability to modulate the spectrum and can in principle reach GHz readout rates. In simulations we extend the spectral range to more than 1000 nm by using a supercontinuum light source, thereby paving the way to various applications requiring high-speed spectroscopic measurements.

https://doi.org/10.1364/OPTICA.424960

1. INTRODUCTION

Spectroscopic techniques are among the most important experimental optical methods, with applications ranging from physics and chemistry to material science and biology [1]. In optical spectroscopy, the change of the frequency spectrum of light due to an interaction with matter allows one to draw conclusions about the properties of a sample. In many cases, the progress in spectroscopic methods was initiated by the emergence of novel states of light interacting with the object under investigation [2].

Over the last decades, various ways have been conceived to structure light in complex manners, which have involved different degrees of freedom, such as the temporal [3] and spatial domain [4]. By correlating different properties, the complexity has further been increased, e.g., by combining time and polarization [5,6], or time and space [7,8]. In the temporal domain, a popular approach to structure light is to shape laser pulses by modulating the frequency spectrum using diffractive elements and spatial light modulators [3]. In the spatial domain, spatial light modulators or similar devices addressing the transverse amplitude of light have been used directly to generate light with a complex transverse structure through amplitude and phase modulation [9]. In both the spatial and temporal domains, the control and understanding over the spatio-temporal shape of light have enabled novel fundamental studies and a myriad of applications. Linking time and polarization brought up new technological opportunities that have been used, for example, in molecular optics [6] and polarimetric measurements [10,11]. Linking frequency and polarization has been used in sensing methods such as spectropolarimetry [12] and spectroscopic ellipsometry [13], e.g., to analyze material properties in astronomy or thin-films. In a more general setting, linking frequency and polarization has also been used to realize wavemeters [14,15].

Among these ways to increase the complexity of the light field, one particularly interesting example is the so-called spatial vector beam. It features a varying transverse spatial amplitude and a varying polarization vector across the beam extent [16–18]. Not only fundamental studies [19,20] and various applications in classical [16,17] and quantum optics [4] of such beams have been of interest, but also analogies between the two domains [21–23]. A recent study shows that strong correlations between the transverse position and polarization in spatial vector beams can be used for high-speed kinematic sensing [24]. There, an object that is moving through the beam in the transverse direction changes the overall polarization of the beam so that simple polarization measurements can be used to track the motion of the object with high speed.

Here, we extend these ideas to the spectral domain and generate states of light that possess a different polarization state for every wavelength. In analogy to the spatial domain, we term these states spectral vector beams (SVBs). We demonstrate that a simple modulation of a femtosecond laser pulse in the time domain using a birefringent crystal enables a controlled and flexible way to generate different polarization patterns across the frequency bandwidth of the light field. We further show that this correlation can be exploited in spectroscopic measurements using only

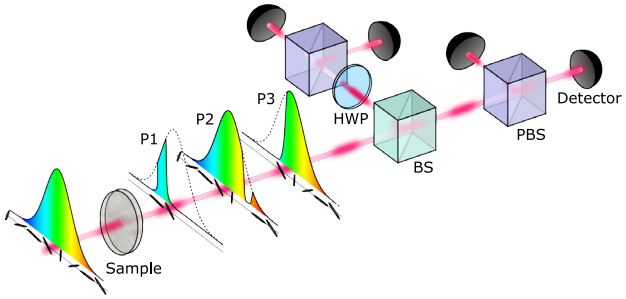

Fig. 1. Conceptual idea. A train of spectral vector pulses propagates through a sample, which could have different absorbing characteristics from pulse to pulse, such as a narrowband transmission (P1), a narrowband absorption (P2), or a long-pass filter (P3). Subsequently, the linear polarization components of the pulses are analyzed using a beam splitter (BS), polarizing beam splitters (PBS), a half-wave plate (HWP), and photodetectors to reconstruct the perturbation of the spectrum. The polarization pattern over wavelength is denoted beneath the spectrum.

polarization measurements, which are generally simpler to measure than the quantities often measured when performing more conventional spectroscopy. Using fast photodiodes, we can track spectral modulations with readout rates of up to 6 MHz, which, in the current experiment, is mainly limited by the speed of our frequency modulation scheme. In general, the presented method can track pulse-to-pulse variations in the frequency spectrum, such that high-speed spectroscopic measurements with GHz readout rates are feasible with current technologies. The general concept is sketched in Fig. 1. Finally, we outline how the spectral measurement range can be extended using coherent supercontinuum light sources, which will allow spectroscopy over the whole NIR or IR spectrum.

2. METHOD

To obtain a polarization state that continuously changes over the frequency spectrum, a light field is required to have a varying relative phase along the frequency spectrum between two orthogonal polarization components. A simple way to realize a continuous phase shift in the frequency domain is to modulate the field in the temporal domain. Here, a time shift τ of the light field translates into a linear phase shift in the frequency domain. Hence, coherently superimposing two orthogonally polarized pulses with a time delay τ gives rise to the wanted correlation between polarization and frequency (i.e., an SVB).

Here, we discuss, without a loss of generality, SVBs for which a linear polarization changes its polarization angle across the frequency range. To generate such beams, two electric fields with an identical envelope $E(t)$ are coherently superimposed. The two fields are circularly polarized, one being right-handed and the other left-handed, and delayed by τ with respect to each other. Using the Jones vector formalism, we can write

$$\vec{E}(t) = \begin{pmatrix} 1 \\ -i \end{pmatrix} E(t) + \begin{pmatrix} 1 \\ i \end{pmatrix} E(t+\tau). \tag{1}$$

By taking the Fourier transform and using the shift theorem, the signal is transposed into the frequency domain:

$$\vec{E}(\omega) = \begin{pmatrix} 1 \\ -i \end{pmatrix} \mathcal{F}[E(t)] + \begin{pmatrix} 1 \\ i \end{pmatrix} e^{-i\omega\tau} \mathcal{F}[E(t)]\,. \tag{2}$$

Thus, the two orthogonal terms of Eq. (1) have a linear phase shift of $\omega\tau$ leading to a rotating linear polarization over frequency, as illustrated in Fig. 1. With an appropriate temporal delay, it is possible to obtain an SVB for which the polarization rotates precisely once over the spectrum. In that case, each linear polarization angle corresponds to one frequency, such that a simple polarization measurement allows conclusions to be drawn about spectral changes without ambiguities. When averaging the signal over time and frequency, the light has a low degree of polarization. For long time delays and nearly no temporal overlap between the two trailing components, the degree of polarization further decreases until it is seemingly unpolarized. We note that the features of SVBs might thus also be interesting from a fundamental point of view. For example, they can be used to investigate analogies between classical and quantum optics [21–23] and to study geometric phases discussed in a similar context in other domains [25,26].

3. RESULTS

A. Generating Spectral Vector Beams

In the experiment, we use a pulsed Ti:Sapphire laser with a pulse duration of around 220 fs and an 80 MHz repetition rate centered around a wavelength of 808 nm. The pulse is diagonally polarized with respect to the optical axis of a birefringent BaB_2O_4 (BBO) crystal. The crystal has different group indices for the horizontally and vertically polarized components $\Delta n_g = -0.12$. Therefore, propagation through the BBO crystal delays the vertically polarized part. A combination of wave plates is then used to convert the wavelength-dependent polarization change to other polarization bases. A sketch of the experimental setup is shown in Fig. 2.

In the first set of experiments, we demonstrate the generation of different SVBs by performing a spectrally resolved polarization tomography using polarization optics and a spectrometer. Here, we use a 2 mm thick crystal to achieve a time delay of roughly the pulse length ($\tau \approx 220\,fs$), which results in a 2π phase ramp over the spectrum of the pulse. The different polarization components of the spectrum are measured with our spectrometer and are used to deduce the polarization states for each wavelength. When superposing two circularly polarized trailing pulses, as described in Eq. (2), a linear polarization that rotates over the spectrum is generated, as shown in Fig. 3(a). SVBs with different polarization patterns can be generated by using different waveplate

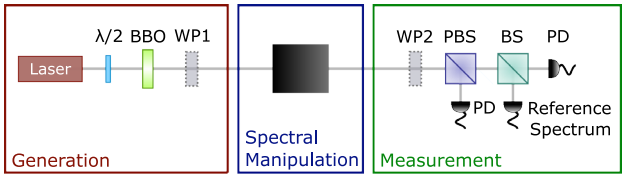

Fig. 2. Sketch of the experimental setup. SVBs are generated using a diagonally polarized pulse whose vertical polarized component is delayed by propagating through a birefringent crystal, such as a BaB_2O_4 (BBO) crystal. A quarter- or half-wave plate (WP1) is used in the generation process to realize different spectral polarization patterns. The spectral components of the pulse are manipulated to replicate different absorption patterns of a sample to simulate spectroscopic measurements. The experimental realizations of these spectral manipulations are displayed in Figs. 4 and 5. Then, a combination of a wave plate (WP2), a polarizing beam splitter (PBS), and photodiodes (PD) are used to project the polarization state into different polarization bases. A measurement using an additional beam splitter (BS) and a spectrometer is used for reference and comparison.

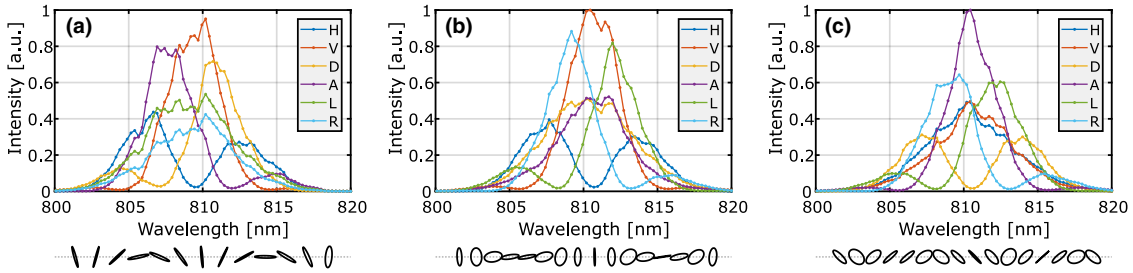

Fig. 3. Measured spectra of three different SVBs with their corresponding polarization patterns, containing only (a) linear polarization and (b) and (c) different linear and circular polarization states. The legend denotes H, V, D, A, L, R for horizontal, vertical, diagonal, antidiagonal, and left- and right-hand circular polarizations, respectively. The spectra are generated by using a half-wave plate, the BBO crystal and additionally either (a) a quarter-wave plate, (b) a half-wave plate, or (c) no wave plate after the BBO crystal (WP1 in Fig. 2). The fast axis of the (a) quarter-wave plate or (b) half-wave plate was adjusted to have an angle of 45° or 22.5° to the vertical polarization axis, respectively.

orientations, which is shown in Figs. 3(b) and 3(c). As described earlier, when averaged over the complete temporal and frequency structure, these beams have a low overall degree of polarization (p). Experimentally, we obtain values $p \approx 0.25$ for the beams presented in Fig. 3. The obtained pattern can be further tuned, e.g., by using crystals of different thicknesses, thereby changing the delay between the two parts of the pulse and the slope of the rotation angle (see Supplement 1). When using SVBs for sensing, this tuning can be used to increase the spectral resolution at the cost of possible ambiguities over the wavelength range. Additionally, the obtained polarization patterns can be spectrally shifted by adding a relative phase between the two superposed parts of the pulse, e.g., through a slight tilt of the birefringent crystal (see Supplement 1).

B. Spectroscopic Measurements

To perform spectroscopic measurements, we use SVBs as described by Eq. (2) and shown in Fig. 3(a). We note that we chose an SVB with only linear polarizations for convenience and technical advantages. The method would work similarly in other polarization bases. We track different spectral manipulations by measuring the change of polarization with only the photodetectors, from which the Stokes parameters are readily obtained (see Supplement 1). At first, the system is calibrated by measuring the Stokes parameters S_1 and S_2 across the whole wavelength range for the unperturbed spectrum with a spectrometer. Then, the crystal width, pulse width, and the phase used in the theoretical simulations is adjusted to match the theoretically predicted spectrum with the experimental one. From the optimized simulations, we can deduce the polarization state over the wavelength. The rotation angle θ of the polarization ellipse is given by

$$\theta = \frac{1}{2} \arctan\left(\frac{S_2}{S_1}\right), \tag{3}$$

and relates S_1 and S_2. Knowing the exact relation between θ and the wavelength allows one to deduce the wavelength by comparing the measured rotation angle with the simulated predictions. We note that for an ideal preparation of this state, the circular polarization components summed up in S_3 always add up to zero. In experiments, imperfect optical elements might lead to a nonzero S_3 value (see Supplement 1). However, they are not considered in the analysis since they do not contribute to the determination of the rotation angle. The polarization measurements are done using silicon photodetectors with a bandwidth of 350 MHz and 50 ps rise times. In general, the simultaneous projections onto two linear polarization bases are necessary to obtain the required Stokes parameters in a single shot measurement, as shown in Fig. 1. In our experiment, we perform the projections onto the two bases consecutively by adjusting a half-wave plate in the measurement setup shown in Fig. 2 accordingly.

To demonstrate the broad range of applicabilities of this method, three different spectral manipulations are simulated: narrowband transmission (P1), narrowband absorption (P2), and a fast varying long-pass filter (P3). These three different measurement scenarios are sketched in Fig. 1. In every approach, the frequency spectrum of the SVB is manipulated by placing the corresponding absorbing masks into the spectral Fourier plane of the beam obtained using the experimental settings depicted on the left in Figs. 4 and 5.

First, we show a polarization measurement tracking the change of the center wavelength of a narrowband transmission. A 210 μm broad slit is placed into the spectral Fourier plane of the pulse, as shown in Fig. 4(a). The movable slit generates a transmission bandwidth of 0.76 nm (FWHM) in the frequency domain, which is on the verge of the resolution of the reference spectrometer specified as 0.7 nm. Different positions of the slit correspond to different center wavelengths of the bandpass filter with invariable bandwidth. Only the polarization components within the transmission bandwidth appear in the subsequent polarization measurements shown in Fig. 4(b). By comparing the measured rotation angle with the simulated predictions based on the calibration spectrum, the center wavelength of the filter is inferred, as shown in Fig. 4(c). The transmission measurements were obtained by averaging up to 80 pulses and have a standard deviation of 0.30 nm averaged over all reconstructed wavelengths. The mean deviation between the reference wavelengths and the inferred center wavelengths is 0.20 nm. The errors are mainly caused by pulse-to-pulse intensity fluctuations of our fs laser. Averaging over several pulses can thus greatly increase the precision at the cost of speed. The narrowband filtering causes a significant increase of $\Delta p = 0.67$ to $p = 0.94 \pm 0.15$ averaged over all measurements. We note that the knowledge of p could also be used to deduce the bandwidth of the filter (see Supplement 1).

In the second set of measurements, a movable wire is placed in the spectral Fourier plane, replicating an absorption line shifting across a wavelength band, as shown in Fig. 4(d). Again, this modulation (i.e., its center wavelength) is tracked through measuring the polarization of the remaining light using Stokes parameters. From

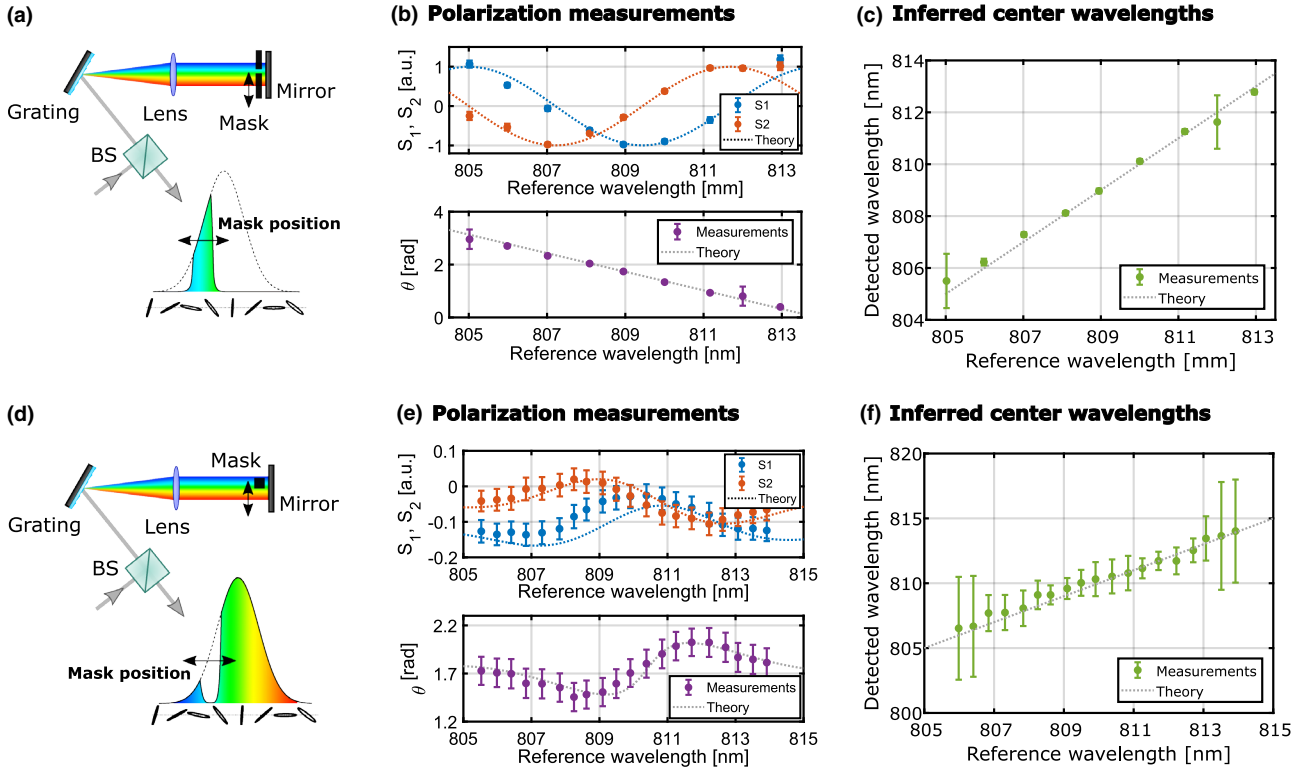

Fig. 4. Spectroscopic measurements using SVBs. (a) Spectral manipulation setup to realize the transmission of a narrow wavelength band, in which a slit is moved through the spectral Fourier plane of the light field. (b) Measured Stokes parameters and the corresponding rotation angle θ derived from the photodetector measurements are plotted over the reference wavelength measured with the spectrometer. (c) Center wavelength of the bandpass filter is inferred from the characterization of the polarization and compared to the reference wavelength. (d) Setup to realize a narrowband wavelength absorption of the spectrum, implemented by placing a wire in the spectral Fourier plane. (e) Measured Stokes parameters and θ as a function of the reference wavelength. (f) Inferred center wavelengths of the narrowband absorption corresponding to the expected values. All errors are obtained by taking the standard deviation of multiple consecutive measurements with the same settings. (a) and (d) BS, Beam splitter.

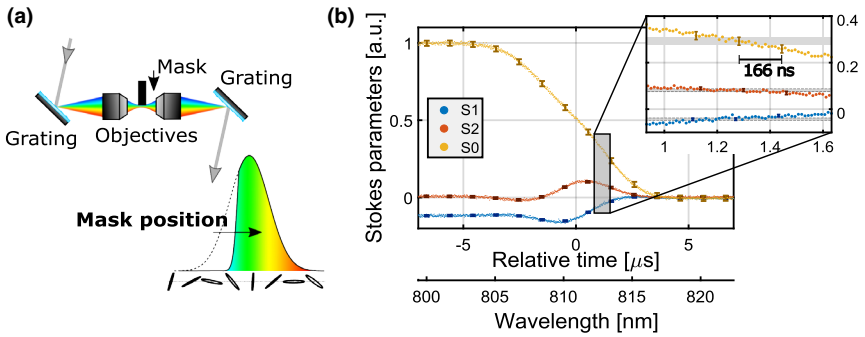

Fig. 5. High-speed tracking of frequency modulations. (a) Spectral manipulation setup for high-speed measurements. A chopper wheel blade is placed in the Fourier plane of a $4f$ system composed of diffraction gratings and two $20\times$ microscope objectives. (b) Stokes parameter measurement tracks the change in polarization, which can be correlated to the absorbed wavelength components. Modulations down to 166.5 ns are resolved within the bounds of the errors.

these values, we deduce the center wavelength of the absorption line. The wire has a diameter of 0.26 mm, mimicking a tunable absorption band with a bandwidth of 1.17 nm in the frequency domain. The absorption is tracked with an averaged standard deviation of 1.84 nm (max. 800 pulses per wavelength), while the mean deviation between the expected wavelength and inferred center wavelengths is 0.34 nm. The larger errors compared to the transmission measurements are caused by the more complex behavior of θ. An additional ambiguity and errors at the extrema of the function, as shown in Fig. 4(e), reduce the precision of the measurement. Finally, the narrowband absorption changes the overall p only slightly by maximally $\Delta p = 0.07$, which shows another challenge in tracking these small changes in the polarization state.

In the final set of experiments, we show the high-speed capabilities of this technique using the setup shown in Fig. 5(a). Here, a chopper wheel blade is placed in the spectral Fourier plane of a $4f$ system composed of two $20\times$ microscope objectives. The mask resembles a time-varying long-pass filter resulting in a constant increase of p and a constant decrease of the overall intensity.

Changes in the spectrum down to 166.5 ns (6 MHz) are resolved within the bounds of the errors. The errors could be significantly reduced with a more stable movable block and a more stable light source. In our implementation, the measuring speed is mainly limited by the speed of our frequency modulation scheme (i.e., a speed of 25.6 m/s with which the chopper wheel passes through the spectrum). Nevertheless, this demonstration shows the potential to measure changes in wavelength with high-speed readout rates, which in principle is only limited by the repetition rate of the laser and the rise time of the electronics. Thus, spectroscopic measurements with GHz readout rates seem accessible when using SVBs.

4. DISCUSSION

One constraint of the current experimental demonstration is the limited spectroscopic range when using ultrashort laser pulses. However, since the presented method in principle works with any pulse shape, broadband applications could use coherent supercontinuum light sources [27]. Simulations using a standard supercontinuum light field suggest the possibility to cover wavelengths from 1000 to 2300 nm (−40 dB bandwidth, see the methods section). Here, the spectrum is polarized and superimposed with its orthogonally polarized and delayed counterpart. A delay of 5.5 fs generates one full π rotation of the polarization across the frequency spectrum (see Supplement 1). With a similar performance as the presented measurements, a resolution of 43 nm seems feasible. The simulated results are shown and discussed in more detail in Supplement 1. Since most materials have a significant birefringence dispersion over such broad wavelength ranges, simply using a birefringent crystal to generate an SVB will result in a complex spectral polarization pattern. Alternatively, using an unbalanced interferometer to generate two orthogonally polarized supercontinuum fields with a slight delay would lead to similarly simple polarization patterns.

5. CONCLUSION

In summary, we demonstrate a simple method to generate spectral vector beams (i.e., light that has a strong correlation between its polarization and wavelength components). Benefiting from this direct correlation, we show that high-speed spectroscopy (e.g., tracking a narrow line absorption or transmission) can be done using only polarization measurements. Because such measurements can be performed with fast photodetectors, the method can track changes of the frequency spectrum with readout rates that are only limited by the repetition rate of the laser and the response time of the detectors (i.e., in the GHz regime). We further outline a way to overcome the limited wavelength range of our light source and describe that a similar method could be applied for broadband spectroscopic sensing using a supercontinuum source.

Besides the experimental implementation of a supercontinuum SVB, it will be interesting to investigate the importance of the degree of coherence [28] and the suitability of broadband incoherent light sources such as LEDs in a similar setting in the future. Thereby, the effect of spectral coherence and low energy densities on SVBs and the presented high-speed spectroscopic method can be investigated. Additionally, it will be important to study extensions of the presented approach to enable the tracking of more complex modulations of the spectrum (e.g., through generating more complex polarization patterns and implementing more advanced signal processing schemes). Moreover, by using a frequency-varying polarization control a time-varying polarization state can be generated that could be useful for ultrafast polarization-gating schemes. Finally, we anticipate that the benefits of the simple generation of SVBs, as well as the spectroscopic method demonstrated here, will stimulate further research into the complex structuring of light, harnessing the spectral and polarization degree of freedom of light.

Funding. Magnus Ehrnrooth Foundation; Väisälän Foundation; Academy of Finland (308596, Academy Research Fellowship—332399, Flagship of PREIN—320165, Strengthen University Research Profiles—301820); Jenny and Antti Wihuri Foundation; National Research Council Canada (High Throughput Secure Networks challenge program, Joint Centre for Extreme Photonics).

Acknowledgment. The authors thank Lauri Salmela for information and data regarding the supercontinuum, and Nikolai V. Tkachenko for fruitful discussions. Authors Lea Kopf, Markus Hiekkamäki and Robert Fickler acknowledge the support of the Academy of Finland through the Competitive Funding to Strengthen University Research Profiles. Lea Kopf also acknowledges support from the Vilho, Yrjö and Kalle Väisälä Foundation of the Finnish Academy of Science and Letters. Markus Hiekkamäki acknowledges support from the Magnus Ehrnrooth Foundation through its graduate student scholarship. Timo Stolt acknowledges the Jenny and Arttu Wihuri Foundation for a Ph.D. fellowship. Frédéric Bouchard acknowledges support from the National Research Council's High Throughput Secure Networks challenge program and the Joint Centre for Extreme Photonics.

Disclosures. The authors declare no conflicts of interest.

Data availability. Data underlying the results presented in this paper are not publicly available at this time but may be obtained from the authors upon reasonable request.

Supplemental document. See Supplement 1 for supporting content.

REFERENCES

1. G. Gauglitz and D. S. Moore, *Handbook of Spectroscopy* (Wiley Online Library, 2014), Vol. **1**.
2. N. V. Tkachenko, *Optical Spectroscopy: Methods and Instrumentations* (Elsevier, 2006).
3. A. Weiner, "Ultrafast optical pulse shaping: a tutorial review," Opt. Commun. **284**, 3669–3692 (2011).
4. H. Rubinsztein-Dunlop, A. Forbes, M. V. Berry, M. R. Dennis, D. L. Andrews, M. Mansuripur, C. Denz, C. Alpmann, P. Banzer, T. Bauer, E. Karimi, L. Marrucci, M. Padgett, M. Ritsch-Marte, N. M. Litchinitser, N. P. Bigelow, C. Rosales-Guzmán, A. Belmonte, J. P. Torres, and T. W. Neely, "Roadmap on structured light," J. Opt. **19**, 013001 (2016).
5. W. J. Walecki, D. N. Fittinghoff, A. L. Smirl, and R. Trebino, "Characterization of the polarization state of weak ultrashort coherent signals by dual-channel spectral interferometry," Opt. Lett. **22**, 81–83 (1997).
6. D. M. Villeneuve, S. A. Aseyev, P. Dietrich, M. Spanner, M. Y. Ivanov, and P. B. Corkum, "Forced molecular rotation in an optical centrifuge," Phys. Rev. Lett. **85**, 542–545 (2000).
7. R. M. Koehl, T. Hattori, and K. A. Nelson, "Automated spatial and temporal shaping of femtosecond pulses," Opt. Commun. **157**, 57–61 (1998).
8. A. M. Shaltout, K. G. Lagoudakis, J. van de Groep, S. J. Kim, J. Vučković, V. M. Shalaev, and M. L. Brongersma, "Spatiotemporal light control with frequency-gradient metasurfaces," Science **365**, 374–377 (2019).
9. A. Forbes, A. Dudley, and M. McLaren, "Creation and detection of optical modes with spatial light modulators," Adv. Opt. Photon. **8**, 200–227 (2016).
10. R. Pinnegar, "Polarization analysis and polarization filtering of three-component signals with the time-frequency *s* transform," Geophys. J. Int. **165**, 596–606 (2006).
11. J. Fade and M. Alouini, "Depolarization remote sensing by orthogonality breaking," Phys. Rev. Lett. **109**, 043901 (2012).
12. J. Iniesta, *Introduction to Spectropolarimetry* (Cambridge University, 2003).

13. D. Aspnes, "Spectroscopic ellipsometry—past, present, and future," Thin Solid Films **571**, 334–344 (2014) [6th International Conference on Spectroscopic Ellipsometry (ICSE-VI)].
14. K. Sano, K. Okada, and K. Hashimoto, "Simple optical wavelength meter in 700–1200 nm wavelength region," Electron. Lett. **16**, 912–913 (1980).
15. T. E. Dimmick, "Simple and accurate wavemeter implemented with a polarization interferometer," Appl. Opt. **36**, 9396–9401 (1997).
16. M. R. Dennis, K. O'Holleran, and M. J. Padgett, "Singular optics: optical vortices and polarization singularities," in *Progress in Optics* (2009), Vol. **53**, pp. 293–363.
17. C. Rosales-Guzmán, B. Ndagano, and A. Forbes, "A review of complex vector light fields and their applications," J. Opt. **20**, 123001 (2018).
18. B. Perez-Garcia, C. López-Mariscal, R. I. Hernandez-Aranda, and J. C. Gutiérrez-Vega, "On-demand tailored vector beams," Appl. Opt. **56**, 6967–6972 (2017).
19. T. Bauer, P. Banzer, E. Karimi, S. Orlov, A. Rubano, L. Marrucci, E. Santamato, R. W. Boyd, and G. Leuchs, "Observation of optical polarization möbius strips," Science **347**, 964–966 (2015).
20. H. Larocque, D. Sugic, D. Mortimer, A. J. Taylor, R. Fickler, R. W. Boyd, M. R. Dennis, and E. Karimi, "Reconstructing the topology of optical polarization knots," Nat. Phys. **14**, 1079–1082 (2018).
21. R. J. Spreeuw, "A classical analogy of entanglement," Found. Phys. **28**, 361–374 (1998).
22. A. Aiello, F. Töppel, C. Marquardt, E. Giacobino, and G. Leuchs, "Quantum-like nonseparable structures in optical beams," New J. Phys. **17**, 043024 (2015).
23. A. Forbes, A. Aiello, and B. Ndagano, "Classically entangled light," in *Progress in Optics* (2019), Vol. **64**, pp. 99–153.
24. S. Berg-Johansen, F. Töppel, B. Stiller, P. Banzer, M. Ornigotti, E. Giacobino, G. Leuchs, A. Aiello, and C. Marquardt, "Classically entangled optical beams for high-speed kinematic sensing," Optica **2**, 864–868 (2015).
25. A. Hannonen, K. Saastamoinen, L.-P. Leppänen, M. Koivurova, A. Shevchenko, A. T. Friberg, and T. Setälä, "Geometric phase in beating of light waves," New J. Phys. **21**, 083030 (2019).
26. A. Hannonen, H. Partanen, A. Leinonen, J. Heikkinen, T. K. Hakala, A. T. Friberg, and T. Setälä, "Measurement of the Pancharatnam–Berry phase in two-beam interference," Optica **7**, 1435–1439 (2020).
27. J. M. Dudley, G. Genty, and S. Coen, "Supercontinuum generation in photonic crystal fiber," Rev. Mod. Phys. **78**, 1135–1184 (2006).
28. A. Luis, "Coherence and visibility for vectorial light," J. Opt. Soc. Am. A **27**, 1764–1769 (2010).